

Electronic Supporting Information

for

**Highly sensitive acetylcholine biosensing via chemical amplification of enzymatic processes in nanochannels**

Yamili Toum Terrones,<sup>1</sup> Gregorio Laucirica,<sup>1</sup> Vanina M. Cayón,<sup>1,2</sup> Gonzalo Fenoy,<sup>1</sup> María Lorena Cortez,<sup>1</sup> María Eugenia Toimil-Molares,<sup>2</sup> Christina Trautmann,<sup>2,3</sup> Waldemar Marmisollé,<sup>1</sup> Omar Azzaroni,<sup>1,\*</sup>

<sup>1</sup>Instituto de Investigaciones Fisicoquímicas Teóricas y Aplicadas (INIFTA), Departamento de Química, Facultad de Ciencias Exactas, Universidad Nacional de La Plata, CONICET – CC 16 Suc. 4, 1900 La Plata, Argentina

<sup>2</sup>GSI Helmholtzzentrum für Schwerionenforschung, 64291 Darmstadt, Germany

<sup>3</sup>Technische Universität Darmstadt, Materialwissenschaft, 64287 Darmstadt, Germany

## Section 1: Experimental Part

### *Chemicals*

KCl, NaOH, HCl and glucose were purchased from Anedra. Acetylcholine chloride ( $\geq 99\%$ ), 4-(2-hydroxyethyl)-1-piperazineethanesulfonic acid ( $\geq 99.5\%$ ) (HEPES), Acetylcholinesterase from *Electrophorus electricus* (electric eel) (Type V-S, lyophilized powder,  $\geq 1,000$  units/mg protein) (AChE), dopamine hydrochloride (DA), serotonin hydrochloride (SA), L-cysteine ( $\geq 97\%$ ) (L-Cys), glucose ( $\geq 99.5\%$ ), L-ascorbic acid ( $\geq 99\%$ ) (AA) and branched polyethyleneimine (Mn=10,000) (PEI) were purchased from Sigma Aldrich. All aqueous solutions were prepared in Milli-Q® water (18.2 M $\Omega$ .cm).

### *PET solid-state nanochannel fabrication (PET SSN)*

Bullet-shaped nanochannels were prepared by the ion track-etching method.<sup>1</sup> The process involves a first step where the PET foils (12  $\mu\text{m}$ , Hostaphan RN 12 Hoechst) are irradiated with a single swift heavy ion ( $\sim 2.2$  GeV Au) at the linear accelerator UNILAC placed at GSI Helmholtzzentrum für Schwerionenforschung (Darmstadt, Germany). Then, in the second step, the irradiated foils are exposed to an asymmetric surfactant-assisted etching, which comprises the exposition of the membranes to concentrated solutions of NaOH for 6 minutes at 60 °C.<sup>2</sup> The asymmetry in the nanochannel shape is given by the different treatment at both openings of the channel: a solution 6 M NaOH was used to generate the larger opening (base side) whereas a small opening (tip side) was achieved by exposing the other side of the membrane to 6 M NaOH with the addition of 0.05% (w/w) Dowfax 2a1. After the etching procedure, the membranes were kept in Milli-Q® water overnight.

### **Nanochannels characterization by Scanning Electron Microscopy (SEM)**

For the SEM characterization of the PET SSN, an irradiated PET foil (fluence of  $10^8$  ions/cm<sup>2</sup>) that had been subjected to an asymmetrical surfactant-assisted etching was positioned at 90°.<sup>2</sup> For the cross-section images, a special freeze-fracture technique was used to render the polymer brittle; in a first step, the membrane is exposed to UV light ( $\lambda_{\text{max}} \sim 315$  nm) for 48 hours to degrade the polymer and make the sample as brittle as glass. Then the sample is broken in liquid N<sub>2</sub> which allows maintaining the original pore structure.<sup>3,4</sup> By treating SEM images with the software Image J®,<sup>5</sup> the base and tip diameters of PET nanochannels were estimated to be  $\sim 600 \pm 28$  nm and  $\sim 85 \pm 7$ , respectively. Also, as shown in **Figure S1**, the channels exhibited a typical bullet profile in the tip region.

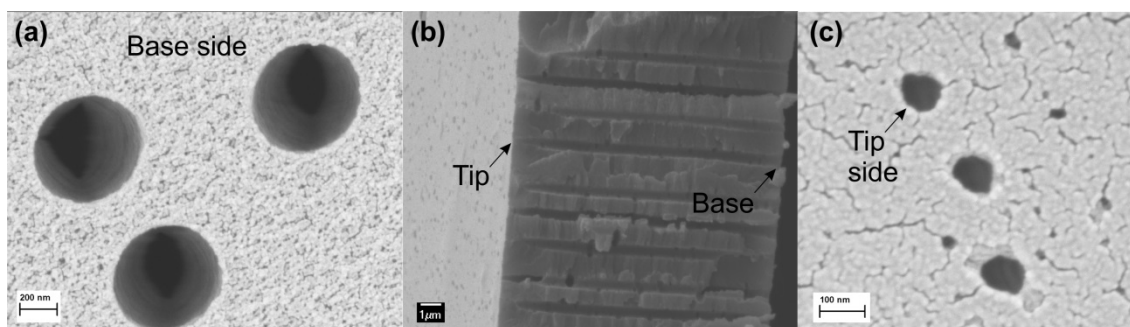


**Figure S1.** SEM micrographs of PET SSN: (a) Base side ( $D \sim 600 \pm 28$  nm), (b) Cross-section where the bullet shape can be noted and (c) Tip side ( $d \sim 85 \pm 7$  nm).

## Channel modification

### 1) PEI immobilization (PET/PEI SSN)

In order to confer positive charge to the nanochannel, the surface was modified with a layer of PEI by electrostatic self-assembly. To this end, the PET membrane containing a nanochannel whose surface bears negatively charged carboxylate groups at  $\text{pH} > 3.5$ , was incubated with a PEI aqueous solution (1 mg/ml) for 2 hours. Then, the modified membrane was rinsed several times with mQ® water.

### 2) AChE immobilization

An AChE stock solution (1 mg/ml) was prepared by dissolving 2 mg of enzyme in 2 ml of KCl 10 mM/ HEPES 0.1 mM and adjusting the pH of the solution to 7.4. Then, taking into account that the isoelectric point of the enzyme is 5.3,<sup>6</sup> using a  $\text{pH} > \text{pI} = 5.3$  ensures a majority of negative charges for the AChE. In order to induce the electrostatic anchoring of the enzyme, 100  $\mu\text{L}$  of the enzyme solution was dropped onto the centre of the PET/PEI membrane (base side, 30 minutes). Next, the same volume was re-used to treat the other side of the membrane (tip side, 30 minutes). Finally, the membrane was rinsed with KCl 10 mM and immediately used for the subsequent experiments.

## Surface Plasmon Resonance (SPR)

Surface Plasmon Resonance (SPR) experiments were carried out by using a SPR Navi 210A instrument (BioNavis Ltd, Tampere, Finland) with a 785 nm laser. Gold sensors (BioNavis Ltd) were employed for SPR were previously cleaned with basic piranha solution. The PEI/AChE assembly was studied by performing two different construction strategies.

In **Construction #1**, a carboxylate-terminated self-assembled monolayer (SAM) was generated by the incubation of the Au substrate in a 5 mM 6-Mercaptohexanoic acid (MHA) solution for 12 h. This self-assembled carboxylic acid layer was employed to emulate the surface of the PET SSN on the Au substrate. Then, the same protocol used for the biosensor construction in the SSNs was followed in real time in SPR. Concretely, a flow-cell was used to inject the polyelectrolyte and enzyme solutions while monitoring the SPR response in real time. Thus, injections of PEI (1mg/ml) and AChE (1mg/ml in 10 mM KCl 0.1 mM HEPES, pH 7.4) were performed separated by buffer injections (10 mM KCl 0.1 mM HEPES, pH 7.4) to *in situ* generate the Au/MHA/PEI/AchE construction. The reflectivity curves were recorded before and after AchE electrostatic anchoring and rinsing with buffer solution (KCl 10 mM, pH 7). The flow rate was 20  $\mu$ L/min for all the experiments, except for the treatment with AchE, when the flow rate was diminished to 1  $\mu$ L/min in order to emulate the conditions used for the immobilization of AchE in the SSN surface. In our configuration, we used a laser source of 785 nm.

In parallel, we performed second strategy (**Construction #2**) in which we anchored PEI (1 mg/ml aqueous solution) directly onto the Au substrate. After AchE (1mg/ml in 10 mM KCl 0.1 mM HEPES, pH 7.4) immobilization, we had the Au/PEI/AchE construction.

From the SPR measurements (sensorgrams and reflectivity curves), we could determine the shift in the angle of minimum reflectivity ( $\Delta\theta$ ) in the SPR response and convert it into mass surface coverage via a calibration constant for this setup as follows

$$Protein\ Surface\ Coverage = \Gamma \left( \frac{ng}{cm^2} \right) = \Delta\theta(degrees) \cdot 1050 \quad (eq. S1)$$

### **Instrumentation for conductimetric measurements**

Conductimetric measurements (*I-V* curves) were carried out in an electrochemical cell using a potentiostat (*Gamry Reference 600*) with a four-electrode arrangement (**Figure S2**). A working electrode W (Pt wire), two reference electrodes WS and R (Ag/AgCl/3 M KCl) and a counter electrode CE (Pt wire) were employed. W and WS electrodes were placed in the chamber facing the tip side of the foil. In a typical experiment, the transmembrane voltage was swept between 1 V and -1 V with a step of 10 mV and a scan rate of 10 mV/s. In all cases, 10 mM KCl was used as supporting electrolyte and, if necessary, the pH value was adjusted by adding HCl and NaOH diluted solutions.

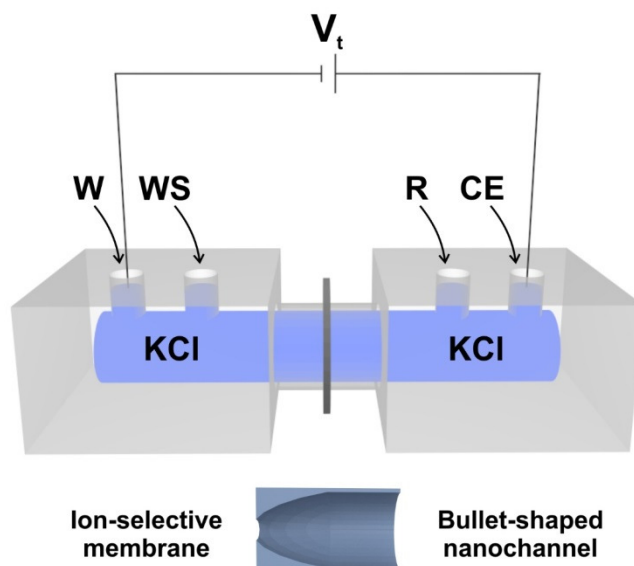


**Figure S2.** Scheme of experimental set-up used for the iontronic (not to scale) measurements consisting of two chambers separated by a PET membrane containing one single bullet-shaped nanochannel. The ionic flow of the KCl electrolyte through the nanochannel is monitored by a potentiostat with four-electrodes (working electrode W, working sense WS, reference R, counter-electrode CE).

### Rectification factor ( $f_{rec}$ )

In order to quantify the rectification efficiency, we calculated  $f_{rec}$  as follows:

$$f_{rec} = \pm \frac{I(-1V \text{ or } 1V)}{I(1V \text{ or } -1V)} \quad (\text{eq. S2})$$

This parameter correlates the response exhibited in the  $I-V$  curves with changes in the surface charge density.<sup>7</sup> This definition implies that the sign of  $f_{rec}$  is determined by the sign of the nanochannel surface charge in the measurement conditions.

## Section 2

### Estimation of the AChE surface coverage by SPR

Using the SPR results (**Figure S3**) and Equation 1 we could calculate the mean protein surface coverage for each construction strategy (**Fig. S3C**). Coverages from both supramolecular constructions are similar, yielding a mean AChE coverage of  $570 \pm 90$  ng/cm<sup>2</sup>. That mean value was calculated by the average of the surface coverage determined by two independent experiments (Construction #1 and Construction #2) reported in **Fig. S3C**.

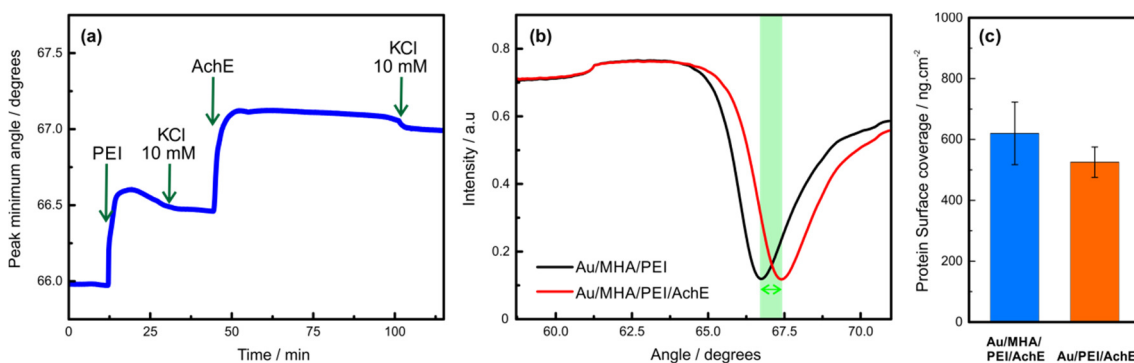


**Figure S3.** (a) Sensogram corresponding to the assembly of the Au/MHA/PEI/AchE construction (Construction #1). (b) SPR curves of the Au/MHA/PEI substrate before and after the enzyme immobilization. (c) Comparison between the surface coverage of AchE obtained by Construction #1 (Au/MHA/PEI/AchE) and Construction #2 (Au/PEI/AchE).

### Reversibility of the PET/PEI nanofluidic response to pH changes

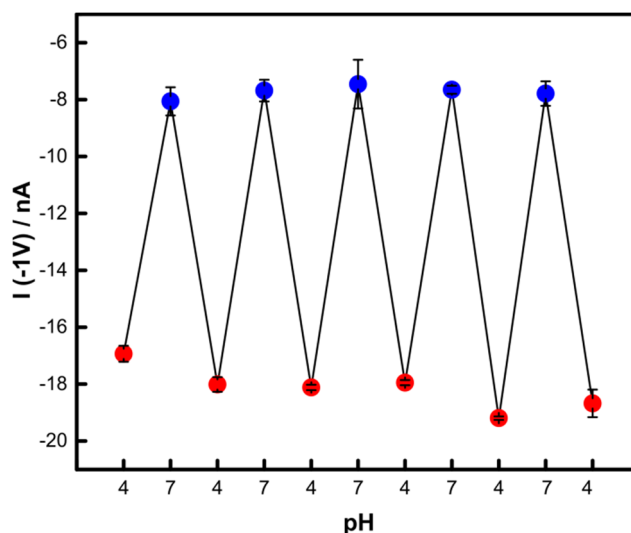


**Figure S4.** Reversibility of the pH response for the PET/PEI SSN. The device was exposed alternatively to solutions containing 10 mM KCl at pH 4 or 10 mM KCl at pH 7. Error bars correspond to three successive measurements in the same conditions.

## pH sensitivity of the nanofluidic response of PET/PEI/AchE nanochannels

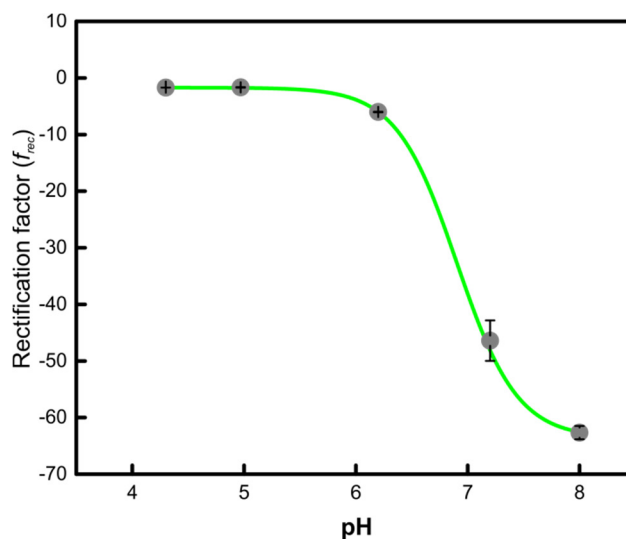


**Figure S5.** Rectification efficiency ( $f_{rec}$ ) versus pH after the modification of the PEI-coated nanochannel with AchE (PET/PEI/AchE SSN). Curves were measured in 10 mM KCl with dropwise addition of NaOH or HCl to reach each pH value. A non-linear regression (Henderson-Hasselbach function) was fitted (green curve) yielding an effective  $pK_a = 6.9 \pm 0.1$ . Error bars correspond to three independent measurements in the same conditions.

## I-V responses of PET/PEI SSN versus PET/PEI/AchE SSN

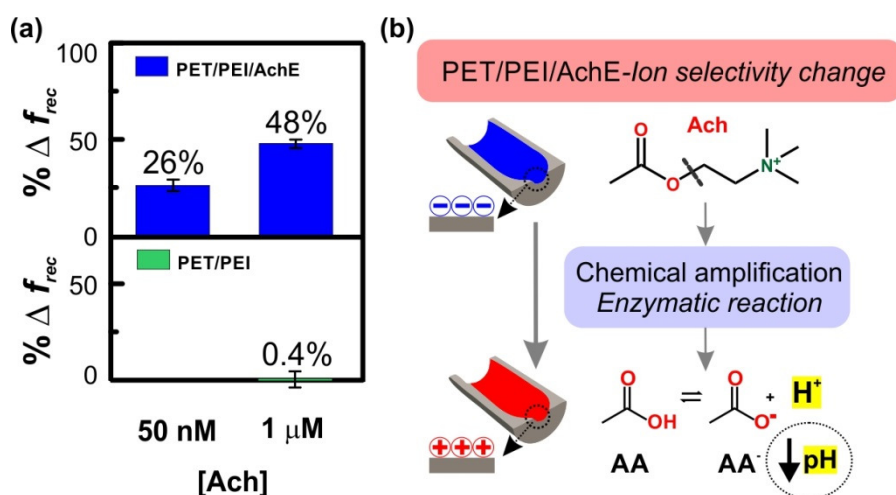


**Figure S6.** (a) Percentage changes in  $f_{rec}$  ( $\% \Delta f_{rec} = [100 \times (|f_{rec0}| - |f_{rec}|) / |f_{rec0}|]$ ) when exposing PET/PEI and PET/PEI/AchE SSNs to different Ach concentrations. Every measurement was carried out in 10 mM KCl and the initial pH was adjusted to 7.  $f_{rec0}$  is the initial  $f_{rec}$  before the exposition to Ach solutions. (b) Scheme depicting the change of the surface charge when the SSNs are exposed to Ach. The enzymatic reaction produces acetic acid (AA), which decreases the local pH causing the protonation of the superficial  $-\text{COO}^-$  groups of PET and makes the surface charge polarity more positive.

## AchE response to acetylcholine in solution

The activity of the enzyme AchE in solution towards Ach was tested by means of measuring the pH change after the addition of Ach. As shown in **Figure S7**, pH decreases from 7 to 4 in the experimental conditions, meaning that the enzyme is active and generates acetic acid that hydrolyses water to form  $H^+$ , decreasing the pH.

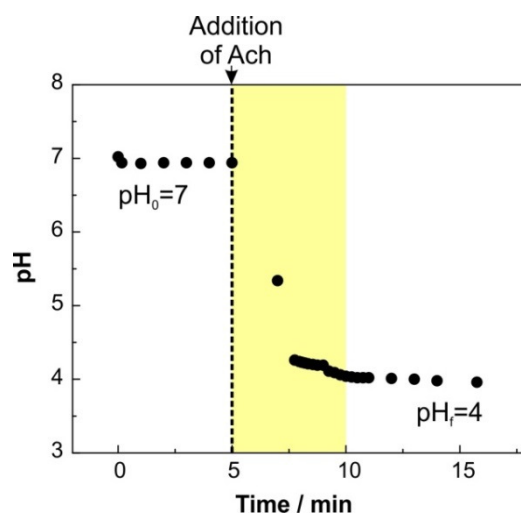


**Figure S7.** Monitoring of the pH decrease upon the addition of 1 mM acetylcholine to a solution of 0.1 mg/ml AchE in 10 mM KCl and 0.1 mM HEPES  $pH_0 = 7.02$ .

## PET/PEI/AchE SSN time response to acetylcholine

An exploration of the ionic transport time-response of the PET/PEI/AchE SSN towards Ach was made to establish an adequate exposition time for all the experiments. As expected, *I-V* curves in **Figure S8(a)** show that, in presence of 100  $\mu\text{M}$  Ach, the ionic transport changes from a cation-selective regime to an anion-driven ionic transport. This means that after 30 minutes of exposure time to 100  $\mu\text{M}$  Ach,  $f_{rec}$  stabilizes (**Figure S8(b)**).

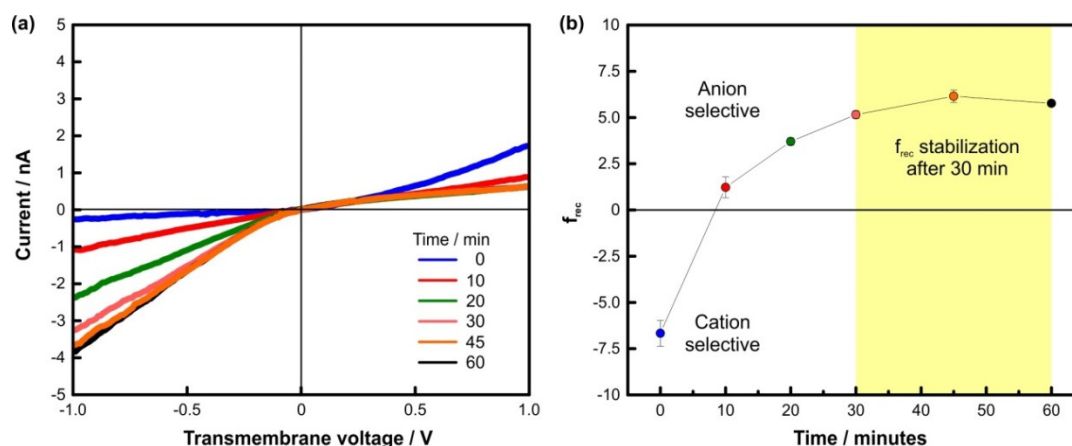


**Figure S8.** (a) PET/PEI/AchE SSN *in situ* *I-V* curves after the nanochannel exposition to a solution 100  $\mu\text{M}$  of acetylcholine in KCl 50 mM (initial pH 7.5) as a function of time (0 to 60 min). (b) Rectification factors calculated from the *I-V* curves for each exposition time (0 to 60 min).

## Comparison between PET/PEI/AchE SSNs and other recently reported enzymatic sensors of Ach

**Table S1.**

Sensor type	Detection range / $\mu\text{M}$	LoD / nM	Recognition element	Ref.
rGo-FET	1-10000	1000	Enzyme AchE	[ <sup>8</sup> ]
rGo-FET	5-1000	2300	Enzyme AchE	[ <sup>9</sup> ]
PET SSN	0.001-25*	16*	Enzyme AchE	Present work

\*Two dynamic ranges were found (linear dependence between  $f_{rec}$  and  $\log([\text{Ach}])$ ). LoD was calculated from the linear regression for the range 0.001-25  $\mu\text{M}$ . The second dynamic ranged was found between 25 and 100  $\mu\text{M}$ .

## Reversibility test

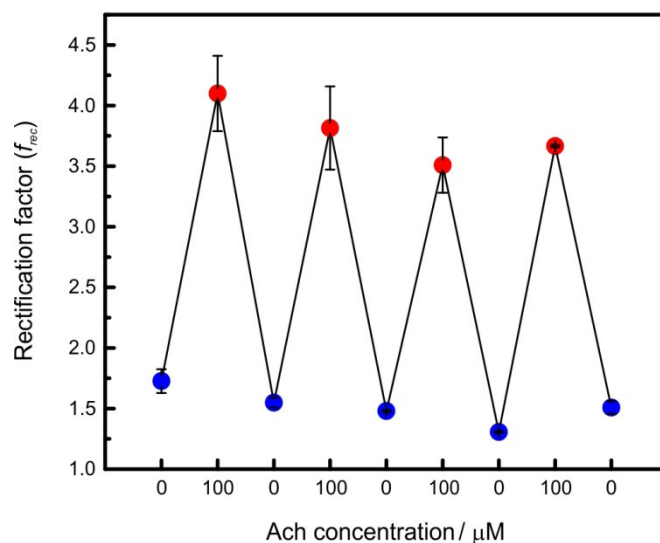


**Figure S9.** Reversibility test for the PET/PEI/AchE SSN. The device was exposed alternatively to solutions containing 10 mM KCl at pH 7 (0  $\mu\text{M}$  Ach) or 100  $\mu\text{M}$  Ach in 10 mM KCl at pH 7. Error bars correspond to three successive measurements in the same conditions.

## Selectivity test

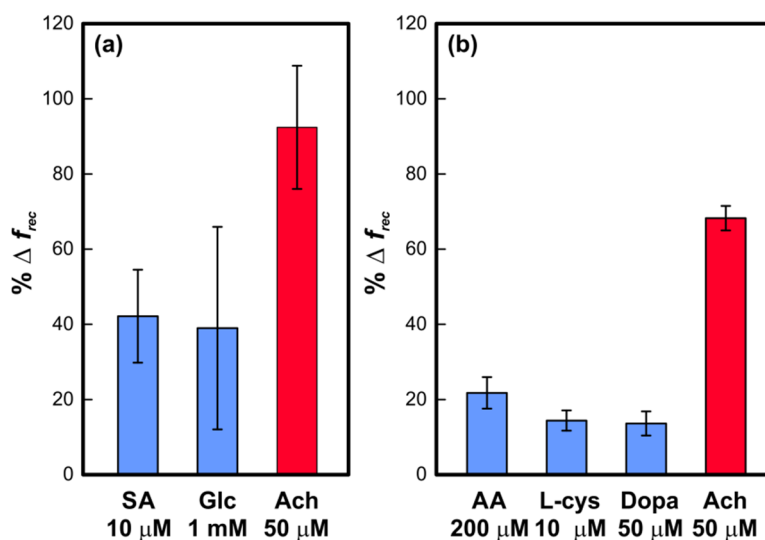


**Figure S10.** Selectivity test in terms of  $f_{rec}$ . Percentage changes in  $f_{rec}$  were calculated as  $\% \Delta f_{rec} = [100 \times (|f_{rec0}| - |f_{rec}|) / |f_{rec0}|]$ , where  $f_{rec0}$  means the rectification efficiency of a solution 10 mM KCl pH 7.  $I-V$  curves were recorded *in situ* (10 mM KCl, pH 7) after the sequential exposure of the channel to: (a) 10  $\mu\text{M}$  serotonin, 1 mM glucose and 50  $\mu\text{M}$  Ach and, (b) 200  $\mu\text{M}$  ascorbic acid, 10  $\mu\text{M}$  L-cysteine, 50  $\mu\text{M}$  dopamine and 50  $\mu\text{M}$  Ach.

## CRediT authorship contribution statement

Yamili Toum Terrones: Conceptualization, Formal analysis, Investigation, Methodology, Writing - original draft. Gregorio Laucirica: Conceptualization, Formal analysis, Investigation, Methodology, Writing - original draft. Vanina M. Cayón: Conceptualization, Investigation. Gonzalo E. Fenoy: Conceptualization, Writing - original draft. M. Lorena Cortez: Conceptualization, Supervision. María Eugenia Toimil-Molares: Conceptualization, Formal analysis, Methodology, Writing - review & editing. Christina Trautmann: Conceptualization, Formal analysis, Methodology, Writing - review & editing. Waldemar A. Marmisollé: Conceptualization, Formal analysis, Investigation, Methodology, Supervision, Writing - original draft. Omar Azzaroni: Conceptualization, Formal analysis, Methodology, Supervision, Writing - review & editing.

## Conflicts of interest

There are no conflicts to declare.

## References

1. Spohr, R. *Ion Tracks and Microtechnology: Principles and Applications*. (Vieweg+Teubner Verlag, 1990).
2. Apel, P. Y. *et al.* Fabrication of nanopores in polymer foils with surfactant-controlled longitudinal profiles. *Nanotechnology* **18**, 305302 (2007).
3. Orelovitch, O. ., Apel, P. Y. & Sartowska, B. Preparation of porous polymer samples for SEM: combination of photo oxidation degradation with a freeze fracture technique. *Mater. Chem. Phys.* **81**, 349–351 (2003).
4. Orelovich, O. L. & Apel', P. Y. Methods for Preparing Samples of Track Membranes for Scanning Electron Microscopy. *Instruments Exp. Tech.* **44**, 111–114 (2001).
5. Schneider, C. A., Rasband, W. S. & Eliceiri, K. W. NIH Image to ImageJ: 25 years of image analysis. *Nat. Methods* **9**, 671–675 (2012).
6. Leuzinger, W., Baker, A. L. & Cauvin, E. Acetylcholinesterase, II. Crystallization, absorption spectra, isoionic point. *PNAS* **59**, 620–623 (1968).
7. Pérez-Mitta, G. *et al.* A Noncovalent Approach towards the Construction of Nanofluidic Diodes with pH-Reversible Rectifying Properties: Insights from Theory and Experiment. *J. Phys. Chem. C* **121**, 9070–9076 (2017).
8. Chae, M.-S., Yoo, Y. K., Kim, J., Kim, T. G. & Hwang, K. S. Graphene-based enzyme-modified field-effect transistor biosensor for monitoring drug effects in Alzheimer's

- disease treatment. *Sensors Actuators B Chem.* **272**, 448–458 (2018).
9. Fenoy, G. E., Marmisollé, W. A., Azzaroni, O. & Knoll, W. Acetylcholine biosensor based on the electrochemical functionalization of graphene field-effect transistors. *Biosens. Bioelectron.* **148**, 111796 (2020).